

Expression of integrin alpha 10 is transcriptionally activated by pRb in mouse osteoblasts and is downregulated in multiple solid tumors

BE Engel¹, E Welsh², MF Emmons¹, PG Santiago-Cardona³ and WD Cress^{*,1}

pRb is known as a classic cell cycle regulator whose inactivation is an important initiator of tumorigenesis. However, more recently, it has also been linked to tumor progression. This study defines a role for pRb as a suppressor of the progression to metastasis by upregulating integrin $\alpha 10$. Transcription of this integrin subunit is herein found to be pRb dependent in mouse osteoblasts. Classic pRb partners in cell cycle control, E2F1 and E2F3, do not repress transcription of integrin $\alpha 10$ and phosphorylation of pRb is not necessary for activation of the integrin $\alpha 10$ promoter. Promoter deletion revealed a pRb-responsive region between – 108 bp to – 55 bp upstream of the start of the site of transcription. pRb activation of transcription also leads to increased levels of integrin $\alpha 10$ protein and a greater concentration of the integrin $\alpha 10$ protein at the cell membrane of mouse osteoblasts. These higher levels of integrin $\alpha 10$ correspond to increased binding to collagen substrate. Consistent with our findings in mouse osteoblasts, we found that integrin $\alpha 10$ is significantly underexpressed in multiple solid tumors that have frequent inactivation of the pRb pathway. Bioinformatically, we identified data consistent with an ‘integrin switch’ that occurs in multiple solid tumors consisting of underexpression of integrins $\alpha 7$, $\alpha 8$, and $\alpha 10$ with concurrent overexpression of integrin $\beta 4$. pRb promotes cell adhesion by inducing expression of integrins necessary for cell adhesion to a substrate. We propose that pRb loss in solid tumors exacerbates aggressiveness by debilitating cellular adhesion, which in turn facilitates tumor cell detachment and metastasis.

Cell Death and Disease (2013) 4, e938; doi:10.1038/cddis.2013.461; published online 28 November 2013

Subject Category: Cancer

The classic pRb pathway comprises pRb, the E2F family of transcription factors, cyclins (primarily D type), cyclin-dependent kinases (CDKs; primarily 4 and 6), and two families of CDK inhibitors (including p16Ink4a). In this classic view, pRb acts as a transcriptional repressor, binding E2F family members at the promoter site of E2F-regulated genes and maintaining transcriptional repression by blocking the transactivation function of E2F and by recruiting additional factors that actively repress transcription.¹ Mitogenic signaling activates the formation of cyclin/CDK complexes, which are responsible for phosphorylating, and thus inactivating, pRb. Once hyperphosphorylated, pRb dissociates from E2F, which is now free to promote the transcription of E2F-regulated genes.

In contrast to its negative regulatory control over E2F-mediated transcription, pRb has also been found to positively regulate the expression of a number of genes. One such gene that was discovered to be positively regulated by pRb is E-cadherin, a cell surface adhesion protein that is a marker for epithelial cells. Both pRb and c-Myc activate transcription of

E-cadherin in the epithelial cells in an AP-2-mediated manner.² Similarly, pRb can bind members of the AP-1 family of transcription factors, including c-Jun, at its AP-1 consensus sequence resulting in stimulation of its transcriptional activity.³ Other genes known to be positively regulated by pRb include the anti-apoptotic gene, Bcl-2, which is activated in an Ap-2-dependent manner⁴ and the CDK inhibitor, p21, which is activated in an Sp1/Sp3-dependent manner.⁵ The transcription factor Sp1 has also been found to be important in the upregulation of integrin $\alpha 5$ through interaction with, and activation by, the transcription factor ZEB2.⁶

pRb is inactivated either directly, through mutation of the *Rb* gene, or indirectly in the majority of human cancers. Cancer types that have a greater than 90% frequency of pRb gene mutation (e.g. retinoblastoma, osteosarcoma, small-cell lung cancer) are also characterized by disrupted cell-to-cell adhesion as mediated by adherens junctions.^{7–9} Previous work has shown that pRb-deficient osteoblasts do not undergo contact-dependent growth arrest, lack adherens junctions, and exhibit altered cadherin expression.¹⁰

¹Molecular Oncology Program, H. Lee Moffitt Cancer Center and Research Institute, Tampa, FL, USA; ²Cancer Bioinformatics Program, H. Lee Moffitt Cancer Center and Research Institute, Tampa, FL, USA and ³Department of Biochemistry, Ponce School of Medicine, Ponce, PR, USA

*Corresponding author: WD Cress, Molecular Oncology Program, H. Lee Moffitt Cancer Center and Research Institute, 12902 Magnolia Drive, Tampa, FL 33612, USA. Tel: +1 813 745 6703; Fax: +1 813 745 7624; E-mail: Douglas.cress@moffitt.org

Keywords: pRb; integrin; oestrosarcoma

Abbreviations: BioGRID, biological general repository for interaction data sets; BSA, bovine serum albumin; CDK, cyclin-dependent kinase; ECL, enhanced chemiluminescence; ECM, extracellular matrix; FBS, fetal bovine serum; MEM- α , minimum essential media α ; NSCLC, non-small cell lung cancer; PBS, phosphate buffered saline; PLS-DA, partial least squares discriminant analysis; pRb, retinoblastoma protein; SDS-PAGE, sodium dodecyl sulfate-polyacrylamide gel electrophoresis

Received 14.5.13; revised 21.10.13; accepted 22.10.13; Edited by A Stephanou

This same work, via microarray, identified a number of genes involved in cell-to-extracellular matrix (ECM) adhesion that may also be pRb regulated. One such gene that was identified was integrin $\alpha 10$.

Integrins are a family of heterodimeric proteins made up of an α and a β subunit. They mediate adhesion of cells to ECM ligands and are unique among transmembrane receptors in that they have the ability to signal bidirectionally, carrying both mechanical and chemical signals.¹¹ Integrin $\alpha 10$ interacts exclusively with the $\beta 1$ subunit to form $\alpha 10\beta 1$ integrin. This is one of four collagen-binding integrins and preferentially binds collagen type IV, the primary collagen type of the basal lamina, but also binds collagens type VI and II, the primary collagen types of the ECM of skeletal muscle and cartilage, respectively.¹² Integrin $\alpha 10$ is found primarily in chondrocytes,^{13,14} but has also been found in chondrogenic mesenchymal stem cells, as well as the endosteum (cell lining between bone marrow and bone) and periosteum (cell lining outside the bone),¹⁵ areas rich in osteoblasts. In these regions, osteoblasts are responsible for bone development and produce osteoid, a matrix composed mainly of collagen type I. A constitutive deletion of integrin $\alpha 10$ in mice resulted in a growth retardation of the long bones while maintaining a normal lifespan and fertility.¹⁶

We hypothesized that not only was integrin $\alpha 10$ present in osteoblasts, but that it was being regulated by pRb. In this article, we demonstrate that pRb transcriptionally activates integrin $\alpha 10$ and that the frequent loss of pRb in multiple solid tumors results in a dramatic downregulation of integrin $\alpha 10$. pRb exerts its tumor-suppressive effect primarily through repressing cell proliferation and inducing a post-mitotic state as well as driving differentiation. We would like to add 'maintaining cellular adhesion to the ECM' as a key tumor suppressive function of pRb as we suspect that the subsequent downregulation of integrin $\alpha 10$ is part of a greater 'integrin switch' that may have a vital role in the development of cancer metastasis. Our study builds upon the growing literature that points to the loss of pRb as a key mediator of the progression to metastasis.

Results

Integrin $\alpha 10$ expression is pRb-dependent in mouse osteoblasts. In previous work, we examined the effects of pRb deficiency in mouse osteoblasts and identified a role for pRb as a regulator of cell adhesion.¹⁰ The microarray screen conducted as part of that work identified integrin $\alpha 10$ as a potential pRb-activated gene. Integrin $\alpha 10$ expression in osteoblasts has not been previously measured, but is known to be high in chondrocytes. Both osteoblasts and chondrocytes are derived from a common progenitor cell so as a first step, we measured the endogenous expression levels of integrin $\alpha 10$ mRNA in mouse osteoblast MC3T3 cells, both wildtype and pRb null, at two different levels of confluency to verify that these cells are integrin $\alpha 10$ positive and that integrin $\alpha 10$ is indeed a pRb target (Figure 1). We found that integrin $\alpha 10$ expression is much higher in pRb wild-type cells as compared with their pRb-null counterparts. Expression levels were also found to be highest at 100% confluency likely due to increased ECM availability at higher cell

densities. The high levels of endogenous integrin $\alpha 10$ and the obvious changes in wild type *versus* pRb-null cells make MC3T3 mouse osteoblast cells an ideal model system to study changes in integrin function and expression engendered by pRb.

Phosphorylation of pRb is not necessary for activation of integrin $\alpha 10$ promoter. We hypothesized that pRb was regulating integrin $\alpha 10$ at the level of transcription. In order to test this, we defined a putative integrin $\alpha 10$ promoter as the 590 base pairs of DNA immediately upstream of the start of the site of transcription using the fully sequenced chromosome 3 from the Mouse Genome Project (NCBI Reference Sequence: NC_000069.6). A variety of constructs were made of this integrin $\alpha 10$ putative promoter (Figure 2) and were determined to be active. When acting as a regulator of cell cycle progression, the phosphorylation status of pRb determines whether or not cells proceed through the G1 checkpoint. Upon phosphorylation by cyclin D/CDK4/6 complexes, pRb becomes inactivated and allows progression to S-phase. To determine if phosphorylation status altered the role of pRb in regulating expression of integrin $\alpha 10$, and to narrow down the minimal responsive region of the integrin $\alpha 10$ promoter, three deletion constructs of the integrin $\alpha 10$ promoter were transfected into MC3T3 cells along with the wild-type pRb large pocket or the non-phosphorylatable pRb large pocket (Figure 3a). Phosphorylation was not necessary for the activation of the integrin $\alpha 10$ promoter. In order to confirm that differences in activation were due to intrinsic properties of the pRb constructs and not due to increased transfection efficiency of either one, a western blot was conducted and the constructs expressed comparable levels of protein (Figure 3b). As a final confirmation that the phosphorylation of pRb is not necessary for upregulation of integrin $\alpha 10$ MC3T3 pRb, wild-type cells were treated with two doses of PD0332991, a drug specific for CDKs 4 and 6, the two CDKs responsible for phosphorylating pRb (Figure 3c). Endogenous levels of integrin $\alpha 10$ mRNA were measured 48 h after application of the drug. Cells treated with the drug did not exhibit any inhibition of integrin $\alpha 10$ mRNA expression as compared with the untreated control cells.

E2F1 and E2F3 do not repress transcription of integrin $\alpha 10$. One of the best characterized roles of pRb is as a regulator of transcription involving its interaction with the E2F family of transcription factors. E2F involvement would likely be the result of the E2F transcription factor repressing transcription of the integrin $\alpha 10$ promoter. Addition of pRb would activate the integrin $\alpha 10$ promoter through alleviating this E2F-mediated repression. Previous studies have identified E2F1 as a repressor of the Mcl-1 promoter.¹⁷ We explored the potential of E2F1 and E2F3 to repress the integrin $\alpha 10$ promoter in the absence of pRb. The addition of E2F1 and E2F3 expression plasmids did not result in repressed transcription (Figure 4) suggesting that pRb is acting through a non-E2F mediated pathway.

Exploring the possible involvement of other transcription factors. According to the Biological General Repository for Interaction Data sets (BioGRID; <http://www.thebiogrid.org>),¹⁸

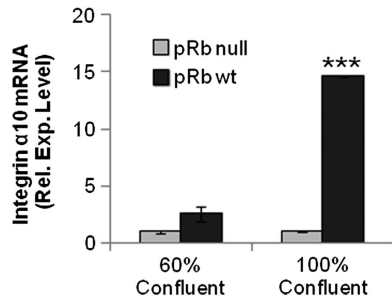


Figure 1 Expression of endogenous integrin $\alpha 10$ mRNA in MC3T3 wild type and MC3T3 pRb-null cells. RNA extraction was performed at two different levels of cell confluency followed by qRT-PCR with integrin $\alpha 10$ -specific primers to determine expression levels relative to GAPDH. The MC3T3 pRb-null expression levels were set as one for each RNA extraction. Asterisk represents significant *P*-value: **P*<0.05

-590 TGTGGGGGA AAGGTGCGGA CACACCATAA TGGTCCCAAT TCAAACAAT
 $\Delta 590$
 -540 CCGTGAACAG CCTCAAGTTA GGGGTGAGAT GTTTTCAACC AAAGTAATTA
 -490 TCTTGACACC ACAAAGCACA CCTGTCTACA GGCAGTGACT CCCCAAAAGC
 $\Delta 463$
 -440 TATTAGACAC ACACAAGCAT GACCATAAAT CAGTGGATTG GCAAGGTCAC
 $\Delta 397$
 -390 ACAGTAGGAC TGCCCTTCAC ACAGTAGGTA GGAAATGCT GCTGTCACTG
 -340 CTGTCAGCTG TTATTTTGA TATCCCATGT TAAGATTAAT AAGGCAAAAA
 $\Delta 275$
 -290 ATATTGTCTC TAAGTCTTAC TTTCTGTTC AACTGGAGG AAATTATTGA
 $\Delta 232$
 -240 ATAAATAAAC CGTGGATAAA AGTAGCCTCA GAAAGGGTCA AAATTGTGT
 $\Delta 163$
 -190 TTTCTTTGAA TATTAGCTGA GGCCTCCAG GGCAGCACC AAGGTAGAGA
 $\Delta 108$
 -140 GCTGGACTAA GGCTGCTCTG TGTCTCTGTC CTGGCTCCC CACAGTCCC
 $\Delta 55$
 -90 TTCACCACC ACTCCATTC CATCCAATT TATTTTATAG TGCCAGTGG
 $\Delta 108$
 -40 AGGGGGCAGG ATAGGAGGGA AAGTAACGAA AACAGCCAAG
 TTTA
 +1 GAGAGGGACA GAGCGACTCA GAGCCTCTCG GACTGGACC GACAAGCGCC
 +51 CATGGAGTCT

Construct	Site-Directed Mutant	Putative TF Binding Site
$\Delta 590$ -YY1	ATATCCCAATGTAAAGATTAAT CCAT -> AACG	-321 to -301
$\Delta 590$ -HBP1 (1)	ATTATTGAATAAATAAACCGTGCAT AATA -> GGCG	-248 TO -224
$\Delta 590$ -PAX6	AATAAATAAACCGTGCATA CCGT -> ATAC	-241 TO -223
$\Delta 590$ -HBP1 (2)	CCACCACCTCCATTCCATCCAA CATT -> ACGC	-88 TO -64
$\Delta 590$ -SP1	GGAGGGGGCAGGATAGG GGC -> TTTA	-42 TO -26

Figure 2 Schematic of the integrin $\alpha 10$ promoter. (a) Schematic shows the eight 5'-nested deletion constructs characterized ($\Delta 590$, $\Delta 463$, $\Delta 397$, $\Delta 275$, $\Delta 232$, $\Delta 163$, $\Delta 108$, $\Delta 55$), the five site-directed mutants of the $\Delta 590$ construct ($\Delta 590$ -YY1, $\Delta 590$ -HBP1(1), $\Delta 590$ -PAX6, $\Delta 590$ -HBP1(2), $\Delta 590$ -SP1) with their four base pair substitutions, the putative transcription factor binding sites (underlined), and the primers used for cloning (highlighted in gray). All constructs begin at the base pair by which they are named (upstream relative to the start of the site of transcription) and end at +60

human pRb associates with 145 unique interactors. Bioinformatic analysis of the integrin $\alpha 10$ promoter was conducted to look for putative binding sites for these 145 interactors using the Genomatix program MatInspector (Genomatix Software GmbH, Munich; <http://www.genomatix.de>; Cartharius *et al.*¹⁹ and Quandt *et al.*²⁰). This analysis

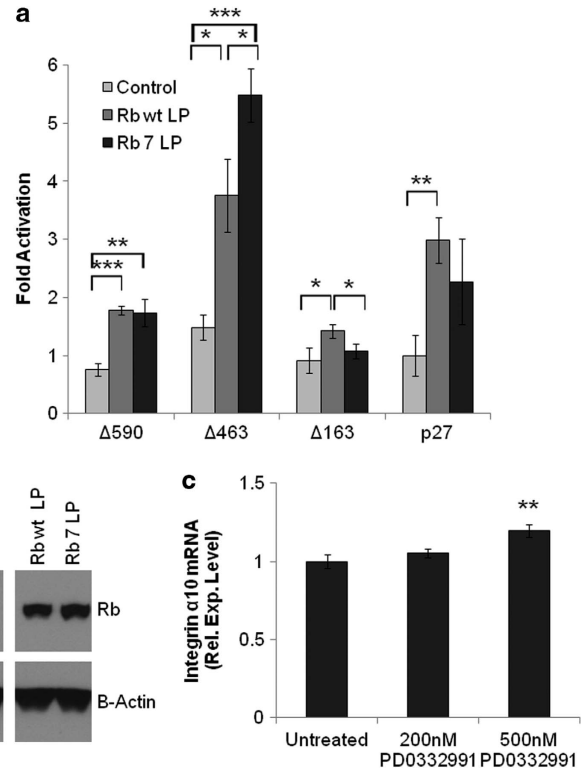


Figure 3 Effect of pRb phosphorylation status on integrin $\alpha 10$ transcription. (a) Three integrin $\alpha 10$ promoter deletion constructs ($\Delta 590$, $\Delta 463$, $\Delta 163$) and a p27 promoter construct control were co-transfected separately with either pEGFPc2 (control), pRb wild type large pocket (Rb wt LP), or pRb non-phosphorylatable large pocket (Rb 7 LP) into MC3T3 pRb-null cells. Promoter activation was measured by luciferase activity. p27 control activity is set to one. (b) Western blot of control (pEGFPc2), pRb wild type large pocket (Rb wt LP), and pRb non-phosphorylatable large pocket (Rb 7 LP) transfected into MC3T3 pRb-null cells. Blot was probed for pRb (9309; Cell Signaling, Boston, MA, USA) and β -Actin (A5441; Sigma). (c) Expression of endogenous integrin $\alpha 10$ mRNA in MC3T3 wild-type cells treated with the CDK 4/6-specific drug, PD0332991 at two different doses (200 nM and 500 nM). RNA extraction was performed 48 h post drug treatment followed by qRT-PCR with integrin $\alpha 10$ -specific primers to determine expression levels relative to GAPDH. The untreated MC3T3 pRb wild type expression levels were set as one. Asterisks represent significant *P*-values as follows: **P*<0.05, ***P*<0.01, and ****P*<0.001

revealed putative transcription factor binding sites for known pRb interacting transcription factors YY1, yin-yang 1, from -321 to -301 bp, HBP1, high-mobility group box transcription factor 1, from -248 to -224 bp (HBP1(1)), PAX6, paired box homeotic gene-6, from -241 to -223, a second HBP1 site from -88 to -64 bp (HBP1(2)), and Sp1, specificity protein 1, from -42 to -26 bp (Figure 2). We decided to further analyze the potential involvement of Sp1 as it is not only known to interact with pRb, but has previously been shown to have a role in the upregulation of integrin $\alpha 5$ along with ZEB2.⁶ Additionally, this site identified on the mouse promoter was also conserved on the human promoter with a putative binding site of base pairs -17 to -1 with respect to the start of the site of transcription (data not shown). We explored the possibility that Sp1 could act with pRb as a co-activator of transcription of the integrin $\alpha 10$ gene. Sp1 was added in the presence and absence of pRb to three integrin $\alpha 10$ promoter constructs in MC3T3 pRb-null

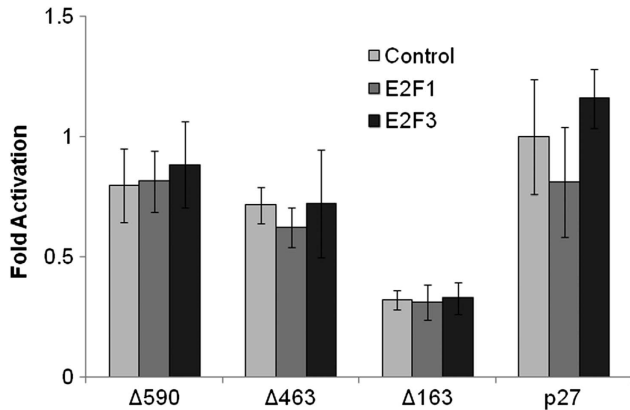


Figure 4 Effect of E2F1 and E2F3 on Integrin α 10 promoter activation. Three integrin α 10 promoter deletion constructs (Δ 590, Δ 463, Δ 163) and a p27 promoter control construct were co-transfected separately with either pEGFPc2 (control), E2F1pcDNA3 (E2F1), or E2F3pcDNA3 (E2F3) into MC3T3 pRb-null cells. Promoter activation was measured by luciferase activity. p27 control activity is set to one. No changes were statistically significant

cells looking for a synergistic activation when both Sp1 and pRb were added; however, no activation was observed to correspond with the addition of Sp1 (data not shown).

As there was no evidence of Sp1 having a role in the activation of integrin α 10, we decided to look at the other putative pRb interacting transcription factor binding sites on the integrin α 10 promoter. Site-directed mutants were made in which the four base pairs most critical for the binding of the transcription factor to the promoter (the 'canonical binding site' as determined by Genomatix) were mutated (Δ 590-YY1, Δ 590-HBP1(1), Δ 590-PAX6, Δ 590-HBP1(2), and Δ 590-Sp1). In addition to the site-directed mutants, a series of progressive deletion mutants were made in which each successive deletion removed one of the putative transcription factor binding sites (Δ 397, Δ 275, Δ 232, Δ 108, and Δ 55). The site-directed mutation of individual binding domains did not reveal a single motif responsible for pRb activation of the integrin α 10 promoter (Figure 5b) pointing to either a lack of individual importance of these transcription factors in the activation of the integrin α 10 promoter, or continued binding despite the mutated base pairs suggesting that they were not, in fact, the canonical binding site. Interestingly, the progressive deletions of the integrin α 10 promoter resulted in progressively diminished transcriptional activation, all the while not losing the activating effect of pRb up until the Δ 55 construct suggesting a pRb responsive region between -108 bp to -55 bp upstream of the start of the site of transcription (Figure 5c).

As all of the constructs and controls are activated by the addition of pRb, a control experiment was conducted using the promoter of CIITA, the class II major histocompatibility complex transactivator, a gene not known to be pRb regulated. As expected, the addition of pRb did not cause any significant change in CIITA transcription (Figure 5a).

pRb wildtype osteoblasts exhibit higher protein levels and adhesion of Integrin α 10 compared with matched pRb-null cells. pRb-activated expression of integrin α 10 mRNA is effectively translated into higher levels of integrin

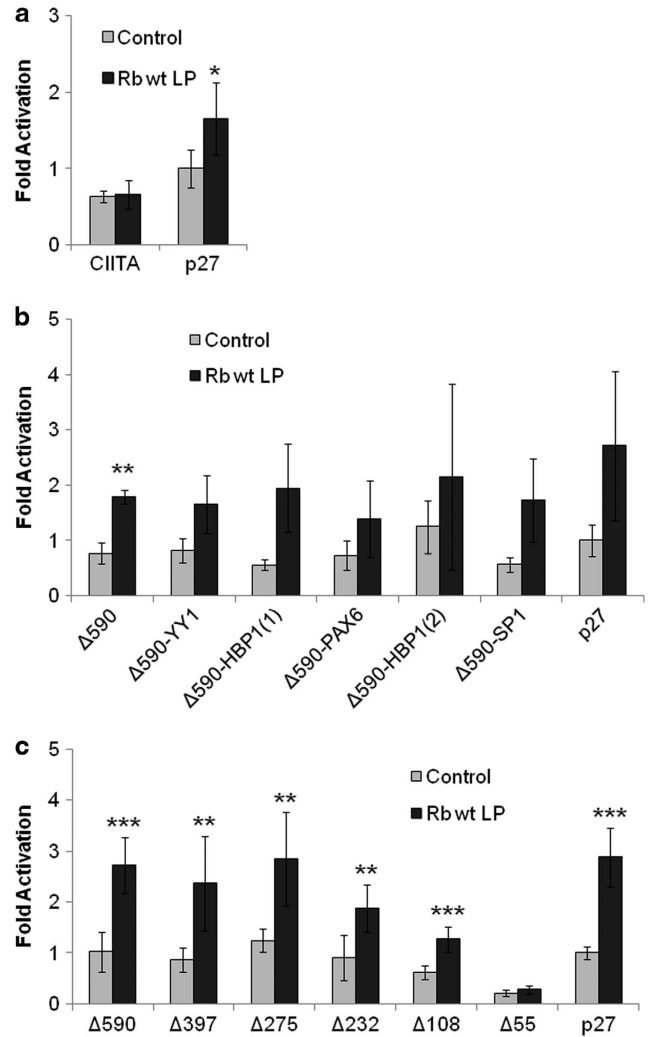


Figure 5 Effect of pRb on activation of site-directed and deletion mutants of the integrin α 10 promoter. (a) A CIITA promoter construct and a p27 promoter control were co-transfected separately with either pEGFPc2 (control) or pRb wild type large pocket (Rb wt LP) into MC3T3 pRb-null cells. Promoter activation was measured by luciferase activity. p27 control activity is set to one. (b) An integrin α 10 promoter construct (Δ 590), five site-directed mutants of that construct (Δ 590-YY1, Δ 590-HBP1(1), Δ 590-PAX6, Δ 590-HBP1(2), Δ 590-Sp1) and a p27 promoter control were co-transfected separately with either pEGFPc2 (control) or pRb wild type large pocket (Rb wt LP) into MC3T3 pRb-null cells. Promoter activation was measured by luciferase activity. p27 control activity is set to one. (c) Six integrin α 10 promoter deletion constructs (Δ 590, Δ 397, Δ 275, Δ 232, Δ 108, Δ 55) and a p27 promoter control were co-transfected separately with either pEGFPc2 (control) or pRb wild type large pocket (Rb wt LP) into MC3T3 pRb-null cells. Promoter activation was measured by luciferase activity. p27 control activity is set to one. Asterisks represent significant P -values as follows: * $P < 0.05$, ** $P < 0.01$, and *** $P < 0.001$

α 10 protein as visualized by immunofluorescence (Figure 6a). Integrin α 10 protein in pRb wild-type osteoblasts is located in high concentrations at the cell membrane forming a well-defined cellular margin. The matched pRb-null osteoblasts are characterized by lower levels of membranous integrin α 10 protein with irregular signal at cell margins. For both cell types nuclear staining with the integrin α 10 antibody is likely nonspecific. No differences in β -tubulin

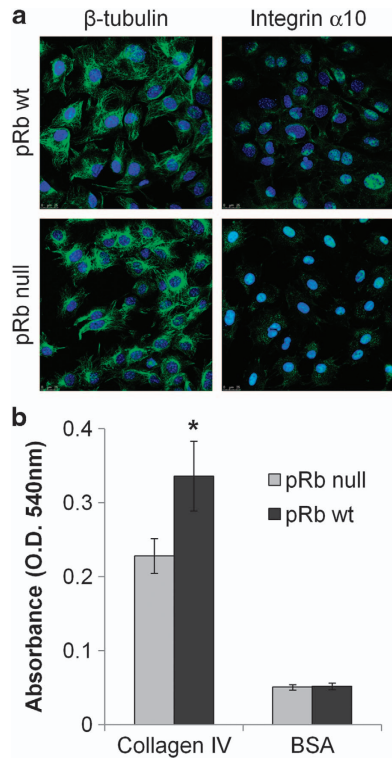


Figure 6 Effect of pRb on Integrin α 10 protein levels and function. (a) MC3T3 pRb wild type and pRb-null cells were probed with antibodies against β -tubulin (2128S; Cell Signaling) and integrin α 10 (AB6030; Millipore, Chicago, IL, USA) (green) and stained with DAPI (blue; nuclei). They were then examined using confocal immunofluorescence microscopy. Representative images are shown. (b) MC3T3 pRb wild type and pRb-null cells were incubated with either collagen IV or BSA substrate and allowed to adhere. Attached cells were permeabilized and stained with crystal violet. Absorbance at 540nm was measured. Asterisk represents significant *P*-value: **P* < 0.05

staining levels and patterns were observed between the two cell lines.

Next, we decided to test the functionality of the integrin α 10 protein in both the pRb wild type and pRb-null osteoblasts. As expected, the higher levels of integrin α 10 protein in pRb wild-type osteoblasts directly corresponded to a statistically significant change of approximately 47% greater binding to collagen IV as compared with matched pRb-null cells (Figure 6b). This indicates that not only is more integrin α 10 protein present in pRb wild-type osteoblasts, but this protein is functional and maintains cellular adhesion to ECM substrate that is lost when pRb is no longer present.

Identification of an ‘integrin switch’ that occurs in multiple solid tumors. Analysis of integrin expression in public databases of the most common solid tumors led to the identification of a four integrin signature that appears as consistently significant changes in mRNA expression levels between tumors and their matched normal tissues. Specifically, the signature consists of overexpression of integrin β 4 and underexpression of integrins α 7, α 8, and α 10 (Table 1, Figures 7a–d). Increased expression of integrin β 4 has also previously been linked to metastasis in human osteosarcoma cells.²¹

Due to the relative rarity of osteosarcoma and the propensity to treat the disease before tumor resection, no data on integrin α 10 expression in tumor and matched normal tissue could be obtained. Instead, seven solid tumor types from the National Cancer Institute’s list of the ten most common solid tumors were examined, including two types of lung cancer, and all exhibited significantly underexpressed integrin α 10 as compared with their matched normal control tissues (Table 1, Figures 7e–h). Specifically, ductal breast carcinoma, the most common type of breast cancer, had the largest fold-change²² (Figure 7g) followed by melanoma²³ (Figure 7h). Squamous cell lung carcinoma, a subtype of non-small cell lung cancer (85% of all lung cancers), which accounts for 25–30% of all non-small cell lung cancers, had the third highest fold-change²⁴ (Figure 7f). Next was superficial bladder cancer, which accounts for 80% of bladder cancers.²⁵ Renal pelvis urothelial carcinoma was next,²⁶ this study also showed downregulation or no change in renal pelvis urothelial cancer in all of the adhesion genes analyzed (e.g. ADAM12, ADAMTS5, ADAM9, TNFAIP6, GNRH2, CD47, CD36, ICAM1, CD96, CD99, SCARB1, CDW52). Sixth was lung adenocarcinoma, which accounts for roughly 50% of all non-small cell lung cancers²⁷ (Figure 7e). Finally, colon mucinous adenocarcinoma was seventh.²⁸

Discussion

In this study, we have demonstrated that integrin α 10 is expressed in mouse osteoblasts and that the expression of this gene is activated at a transcriptional level by pRb. This activation of expression directly leads to increased integrin α 10 protein levels and greater adhesion to a collagen substrate. Our analysis of publically available databases revealed that integrin α 10 is significantly downregulated in tumor tissue compared with normal in multiple solid tumors. These findings point to an important role for changes in integrin α 10 expression during disease progression.

pRb’s activation of integrin α 10 occurs in a non-classical manner in which E2Fs are not involved, and the phosphorylation status of pRb does not have a role. This is in agreement with previous studies, which have shown that pRb mutants associated with a low risk of retinoblastoma retained the ability to activate transcription suggesting dual tumor suppressor functions linked to cell cycle progression and differentiation.²⁹ pRb mutants that can no longer bind E2F and prevent cell cycle progression, but are still able to activate transcription of target genes, including integrin α 10, are associated with lower risk of cancer and better overall survival.

The downregulation of integrin α 10 following pRb loss may be part of a larger oncogenic event in which cellular differentiation is lost. Differentiation has previously been measured as part of a ‘cadherin switch’ in which epithelial cells lose their epithelial phenotype and become more mesenchymal in character. We propose that there is a simultaneous ‘integrin switch’ involving the downregulation of integrins α 10, α 7, α 8, and potentially other positive prognostic integrins with concurrent upregulation of less favorable integrins, including integrin β 4, that results in a loss of adhesion to the local extracellular matrix allowing previously anchored cells to metastasize. As a highly

Table 1 Oncomine (<http://www.oncomine.org>, Compendia Bioscience, Ann Arbor, MI, USA) was used for analysis of integrin expression in seven common solid tumor types

Database	Integrin $\alpha 7$		Integrin $\alpha 8$		Integrin $\alpha 10$		Integrin $\beta 4$	
	Fold Change	P-value	Fold Change	P-value	Fold Change	P-value	Fold Change	P-value
Dyrskjot Bladder 3	-1.587	-1.63E-05	-1.475	2.25E-04	-1.604	3.99E-07	2.313	1.82E-05
Haqq Melanoma	NC	2.68E-01	-1.504	3.00E-03	-3.471	2.04E-04	N/A	N/A
Hou Lung	-1.734	1.64E-14	-5.742	1.91E-15	-1.828	2.88E-18	3.591	8.92E-10
Jones Renal	-1.523	2.45E-05	-3.993	7.00E-17	-1.499	5.91E-10	2.500	2.00E-03
Kaiser Colon	NC	9.40E-02	-1.494	1.00E-03	-1.222	6.09E-06	2.852	5.81E-05
Landi Lung	-1.239	1.01E-07	-2.375	4.58E-17	-1.357	9.02E-14	1.588	3.36E-07
Richardson Breast	-5.362	3.41E-06	NC	1.70E-02	-3.491	2.00E-06	-2.735*	1.86E-08

The fold change value is determined by comparing the means of the two classes in an analysis on a log2 scale and then converting that difference to a linear scale (<http://www.oncomine.org>). NC, no significant difference in expression between normal and tumor tissue. N/A, this study did not have a probe for the gene of interest. Only one significant change occurred in the opposite direction of the other six data sets and is denoted with an asterisk

tissue-specific integrin, loss of $\alpha 10$ may be associated with a loss of differentiation. There is potential to use integrin $\alpha 10$ levels as a prognostic marker. High levels indicate a tumor that has retained differentiation and will likely have better overall survival while decreased expression levels are an indicator of a more advanced disease state in which pRb has been lost or mutated.

This study builds upon our previous work defining a role for pRb as a regulator of mouse osteoblast cell adhesion¹⁰ and adds to the growing literature that links pRb to the metastatic cascade.³⁰

Materials and Methods

Cell lines and drug treatment. Cell lines and the mice they were derived from were previously described by Sosa-Garcia *et al.*¹⁰ Briefly, primary osteoblasts were isolated and 3T3 immortalized from *Rb1* conditional knockout embryonic mice and their Rb wild-type littermates to produce pRb-null and pRb wild-type MC3T3 cell lines, respectively. They were grown in Minimum Essential Medium Alpha (MEM- α) supplemented with 10% fetal bovine serum (FBS) and 1% penicillin/streptomycin. Approximately 2×10^6 MC3T3 Rb wild-type cells were cultured in p60 plates and received either a control treatment (complete media) or a drug treatment consisting of complete media supplemented with either 200 nM or 500 nM of the CDK 4/6-specific inhibitor, PD0332991 (ChemTek, Indianapolis, IN, USA). Cells were harvested 48 h after treatment and underwent RNA extraction followed by QRT-PCR as described below.

Plasmid vectors. The pGL3-p27,³¹ Rb wt LP, Rb 7 LP,³² pEGFPc2 (GenBank Accession #U57606), pcDNA3-E2F1,¹⁷ pcDNA3-E2F3,³³ CMV-Sp1(Plasmid 12097 purchased from <http://www.addgene.org>), and pGL3-CIITA- $\Delta 195$ (Gift from Ken Wright, Moffitt Cancer Center; Ghosh *et al.*³⁴) have all been previously characterized. The novel promoter plasmids were generated by PCR using the following primers: $\Delta 590$ forward (5'-GAGAGGTACCTGTTGGGGGAAA GGTGCGGA-3'), $\Delta 463$ forward (5'-GAGAGGTACCACAGGCAGTGACTCCCCAAA GC-3'), $\Delta 397$ forward (5'-GAGAGGTACCAGGTACACAGTAGGACTGCC-3'), $\Delta 275$ forward (5'-GAGAGGTACCCTACTTTCTGTTCCAACTGGAGG-3'), $\Delta 232$ forward (5'-GAGAGGTACCACCGTGCATAAAAGTAGCCTCAGAA-3'), $\Delta 163$ forward (5'-GAGAGGTACCAGGGGCGAGCAACAAGGTAGAG-3'), $\Delta 108$ forward (5'-GAGAGGTACCGGCTCCCCACAGCTCCCTTC-3'), $\Delta 55$ forward (5'-GAGAGGTACCTTAGCTGCCAGTGGGAGGGG-3'). Reverse primer for all of the aforementioned (5'-GAGAAGATCTAGACTCCATGGGCGCTTGCC-3'). The products were cleaved with KpnI and BglII and cloned into those sites of the pGL3-basic vector (Promega, Chicago, IL, USA). Site-directed mutants were created using the $\Delta 590$ plasmid altered with the following internal mutational primers and their reverse complements as reverse primers: $\Delta 590$ -YY1 forward (5'-GTTAT TTTGCATATCAACGGTTAAGATTAATAAG-3'), $\Delta 590$ -HBP1(1) forward (5'-TGGA GCAAATTTATGGGCGAATAAACCGTGCATA-3'), $\Delta 590$ -PAX6 forward (5'-TATT GAATAAATAAACACGCATAAAAGTAGCCT-3'), $\Delta 590$ -HBP1(2) forward (5'-TTC CACCACCCTCCACGCCATCCAACCTTTATT-3'), $\Delta 590$ -SP1 forward (5'-GCTG CCAGTGGGAGGTTAAGGATAGGAGGGAAA-3').

Luciferase assays. Approximately 100 000 cells per well of MC3T3 Rb-null cells were cultured in 24-well plates and transfected with a mixture containing 500 ng promoter construct, 50 ng Renilla luciferase reporter (pRL-TK, Promega), and 2.5 μ g of either Rb expression plasmid or empty control vector (pEGFPc2) for an equal amount of DNA diluted in 100 μ l serum-free MEM- α for each transfection. One microliter X-tremeGENE HP DNA transfection reagent (Roche Diagnostics, Indianapolis, IN, USA) was added to the DNA mixture and allowed to incubate for 20 min before being added to the MC3T3 Rb-null cells to a total volume of 600 μ l (500 μ l serum-free medium plus 100 μ l transfection mixture). Cells were incubated with the transfection mixture for 4 h before being returned to complete media (MEM- α plus 10% FBS, 1% penicillin/streptomycin). Cells were harvested 48 h after transfection and luciferase assays were performed using the dual-luciferase reporter assay system (Promega) following the manufacturer's protocol and read using a 20/20¹ Luminometer (Turner Biosystems, Sunnyvale, CA, USA) with standard promega protocol DLR-O-INJ. Experiments were done in triplicate. To control for transfection efficiency, firefly luciferase values were normalized to the values for Renilla luciferase.

Quantitative real-time PCR. Total cell RNA was harvested using the RNeasy Mini Kit (Qiagen, Carol Stream, IL, USA) following the manufacturer's instructions. Reverse transcription reactions were carried out using iScript cDNA Synthesis Kit (Bio-Rad, Chicago, IL, USA). Real-time PCR was performed using Bio-Rad iQ SYBR Green Supermix on a CFX96 real-time PCR detection system (Bio-Rad). The following primers were used: Itg $\alpha 10$ forward (5'-GGCTCCAACAGT ATCTATCC-3'), Itg $\alpha 10$ reverse (5'-TGCTCTCACAACCTCTTCC-3'), GAPDH forward (5'-AACGACCCCTTCATTGAC-3'), GAPDH reverse (5'-CTCCACGACATA CTCAGCAC-3').

Western blotting. Western blots were performed as previously described.³⁵ Briefly, cell lysates were normalized for total protein content (35 μ g) and subjected to SDS-PAGE. Detection of proteins was accomplished using horseradish peroxidase-conjugated secondary antibodies and enhanced chemiluminescence (ECL; Amersham Biosciences, GE Life Sciences, Pittsburgh, PA, USA). Antibodies used include a mouse monoclonal antibody specific for endogenous pRb residues 701-928 (9309; Cell Signaling), a goat polyclonal antibody corresponding to amino acids 528-546 of Sp1 (sc-59-G; Santa Cruz Biotechnology), and a mouse monoclonal β -actin antibody (A5441; Sigma).

Immunofluorescence. Immunofluorescence was performed as previously described³⁶ without permeabilization. Briefly, cells were seeded in a Lab-Tak eight-chamber slide (Thermo Scientific, Waltham, MA, USA) 1 day before experimentation. They were rinsed with PBS and fixed in 4% paraformaldehyde followed by neutralization with glycine. Cells were then sequentially incubated in 10% bovine serum albumin (BSA), either anti-integrin $\alpha 10$ (AB6030; Millipore) or anti- β -tubulin (2128S; Cell Signaling), followed by secondary AlexaFluor 488-conjugated goat anti-rabbit antibody (Invitrogen, Life Technologies, Grand Island, NY, USA) with added DAPI. This was followed by washing three times in PBS and covering the wells with Vectashield mounting media (Vector Labs, Burlingame, CA, USA) and coverslips. Cells were imaged by the Moffitt Cancer Center Microscopy Core with a Leica SP5, Chicago, IL, USA AOBs tandem scanning inverted confocal microscope.

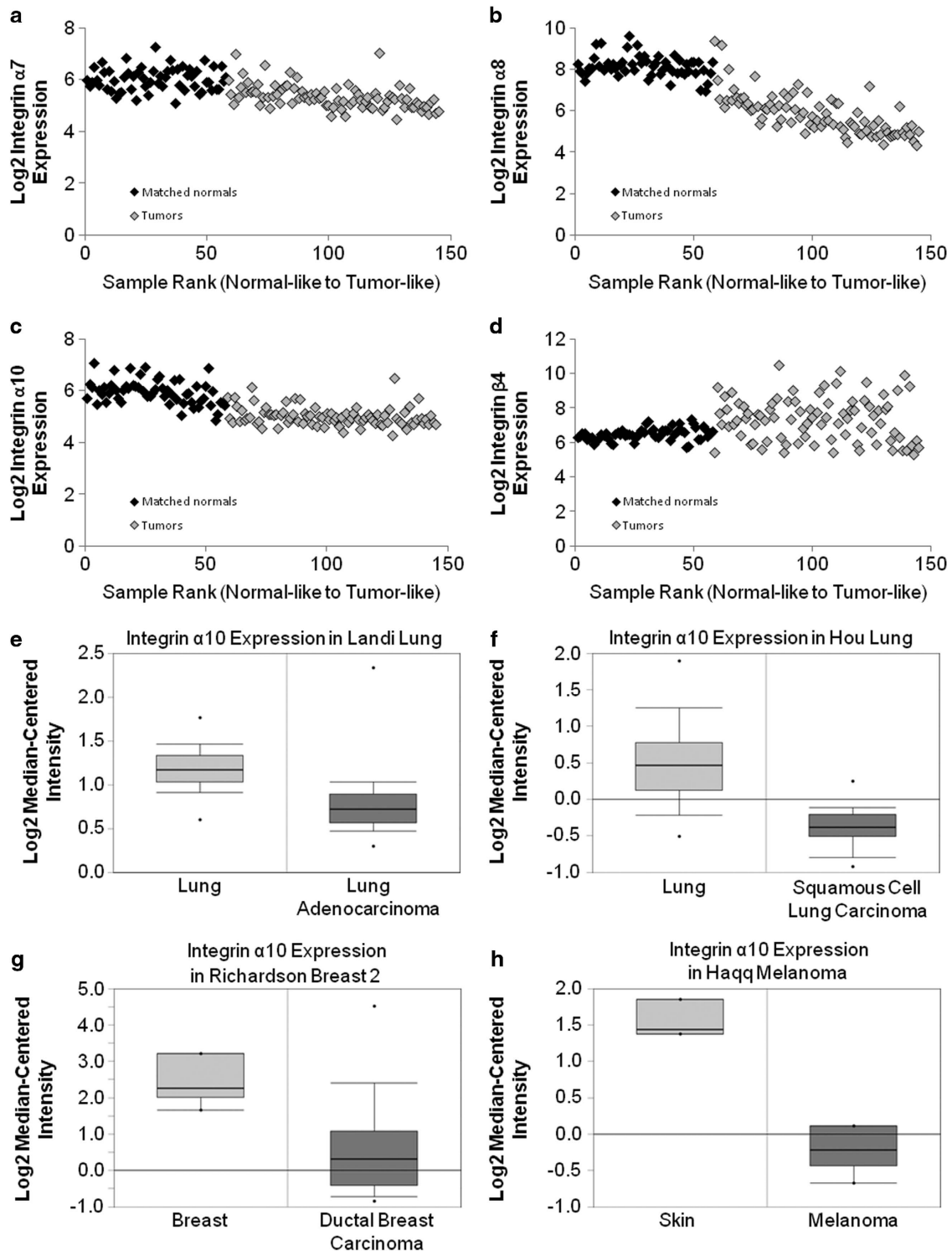


Figure 7 Changes in integrin expression occur in multiple solid tumors. (a–d) The GSE19188 data set of NSCLC tumor and adjacent normal samples was ranked from most normal to most tumor like. Samples 1–58 are the adjacent normals (black diamonds) whereas samples 59–145 represent tumor samples (light gray diamonds). Gene expression was determined via microarray for integrin $\alpha 7$ using probe 216331_at (a), $\alpha 8$ using probe 214265_at (b), $\alpha 10$ using probe 206766_at (c), and $\beta 4$ using probe 204990_s_at (d). (e–h) Oncomine (<http://www.oncomine.org>, Compendia Bioscience, Ann Arbor, MI, USA) was used for analysis and visualization of integrin $\alpha 10$ expression in four common solid tumor types. Data sets were ordered by underexpression: P -value of $Itg\alpha 10$. (e) Analysis of integrin $\alpha 10$ expression in normal lung ($n = 49$) versus lung adenocarcinoma ($n = 58$) from the Landi Lung database. (f) Analysis of integrin $\alpha 10$ expression in normal lung ($n = 65$) versus squamous cell lung carcinoma ($n = 27$) from the Hou Lung database. (g) Analysis of integrin $\alpha 10$ expression in normal breast ($n = 7$) versus ductal breast carcinoma ($n = 40$) from the Richardson Breast 2 database. (h) Analysis of integrin $\alpha 10$ expression in normal skin ($n = 3$) versus melanoma ($n = 6$) from the Haqq Melanoma database

Functional adhesion assays. Functional adhesion assays were performed as previously described.³⁷ Briefly, 96-well Immunosorp (Nunc, Sigma Aldrich, St Louis, MO, USA) plates were coated with either 50 μ l (40 μ g/ml) of soluble Cultrex mouse collagen IV (BD Biosciences, San José, CA, USA) or BSA and allowed to evaporate overnight at room temperature. Cells were washed once in serum-free MEM- α and resuspended at a density of 1×10^6 cells/ml with 1×10^5 cells added to each well. After 2 h of adhesion, unattached cells were removed by three washes with MEM- α , and adherent cells were fixed with 70% methanol for 10 min, dried, and subsequently stained with a solution of 0.02% crystal violet at 0.2% ethanol. The stained cells were solubilized in 100 μ l Sorenson solution and absorbance was read at 540 nm with an automated 96-well plate reader (VERSAmix, Sunnyvale, CA, USA). Mean and SE values were calculated from the results in four independent wells. Experiments were repeated three times and results of representative experiments are shown.

Mining public databases. Microarray studies conducted on cancers included in the National Cancer Institute's list of the 10 most common solid tumors (bladder, breast, colon and rectal, endometrial, kidney (renal cell), lung, melanoma, pancreatic, prostate, thyroid; <http://www.cancer.gov/cancertopics/types/commoncancers>) were analyzed using OncoPrint (<http://www.oncoPrint.org>, Compendia Bioscience, Ann Arbor, MI, USA). Data sets were ordered by under- or overexpression: *P*-value of integrin analyzed. All known integrins with corresponding probesets were analyzed including integrins α 1-11, α 2B, α L, α M, α X, α V, α E, β 1-8, and β L1. The only integrins found to be significantly under- or overexpressed in at least five of the seven data sets were integrins α 7, α 8, α 10, and β 4. These four integrins were further analyzed using seven previously published microarray studies²²⁻²⁸ to evaluate their mRNA expression. Six studies used Affymetrix human genome arrays with the probe set 216331_at for integrin α 7, 214265_at for integrin α 8, 206766_at for integrin α 10, and 204990_s for integrin β 4 with the exception of the Kaiser study, which used probe set 211905_at for integrin β 4. The seventh study by Haqq et al.²³ used a microarray of 20 862 cDNA targets representing 19 740 unique genes (Research Genetics, Huntsville, AL, USA) with the probe set H44722 for integrin α 10, and R87964 for integrin α 8. The study by Dyrskjot et al.²⁵ included nine samples of normal bladder and five samples of normal bladder mucosa as well as 28 samples of superficial bladder cancer (superficial transitional cell carcinoma) comprising 15 tumor biopsies without surrounding carcinoma *in situ* and 13 tumor biopsies with surrounding carcinoma *in situ*. The study by Haqq et al.²³ included three samples of normal skin and six samples of melanoma. The study by Hou et al.²⁴ included 65 samples of normal lung and 27 samples of squamous cell lung carcinoma. The study by Jones et al.²⁶ included 23 samples of normal kidney and eight samples of renal pelvis urothelial carcinoma (transitional cell cancers of the renal pelvis). The study by Kaiser et al.²⁸ included five samples of normal colon and 13 samples of colon mucinous adenocarcinoma. The study by Landi et al.²⁷ included 49 samples of normal lung and 58 samples of lung adenocarcinoma. The study by Richardson et al.²² included seven samples of normal breast and 40 samples of ductal breast carcinoma.

Statistical methods. A data set of non-small cell lung cancer (NSCLC) tumor and adjacent normal samples (GSE19188) was used to identify genes differentially expressed between tumor and adjacent normal. Sample GSM475805 was identified as a corrupt CEL file and excluded from all analyses. Data were normalized with the RMA algorithm using the libaffy software,³⁸ and principle component analysis (PCA) was performed on the remaining 155 samples, using the Evinced software (UmBio AB, Umeå, Sweden), to identify outliers. Three tumor samples (GSM475677, GSM475706, GSM475780) clustered in the middle of the adjacent normal samples, and one adjacent normal sample (GSM475666) fell within the tumor distribution. These samples were discarded for all further tumor versus adjacent normal analysis. An additional six outlier adjacent normal samples (GSM475752, GSM475755, GSM475766, GSM475781, GSM475807, GSM475811) were identified as falling outside the otherwise tight adjacent normal distribution, lying between the adjacent normal and tumor clusters. Subsequent analyses (data not shown) confirmed that these samples exhibit a more tumor-like gene expression profile than the other adjacent normals, and were thus discarded from further tumor versus adjacent normal analysis. The final tumor plus adjacent normal data set, after discarding outliers, consisted of 58 adjacent normal and 87 tumor samples. Samples were then ranked by their respective scores from the first principle component of a partial least squares discriminate

analysis (PLS-DA) model, trained on tumor versus adjacent normal, to order them from most normal-like to most tumor-like global gene expression.

Statistical significance of data was calculated using a two-tailed Student's *t*-test in Microsoft Excel.

Conflict of Interest

The authors declare no conflict of interest.

Acknowledgements. We would like to thank L Chen for statistical analysis, J Johnson for microscopy assistance, and E Knudsen and K Wright for sharing plasmids. This work was supported by NCI Grants CA119997 (WDC), CA163068 (WDC and PGS), CA118809 (WDC and PGS), DOD Grant W81XWH (WDC and EW), a USF Presidential Fellowship (BEE) and the Moffitt Cancer Center.

- Knudsen ES, Wang JYJ. Targeting the RB-pathway in cancer therapy. *Clin Cancer Res* 2010; **16**: 1094–1099.
- Batsche E, Muchardt C, Behrens J, Hurst HC, Cremisi C. RB and c-Myc activate expression of the E-cadherin gene in epithelial cells through interaction with transcription factor AP-2. *Mol Cell Biol* 1998; **18**: 3647–3658.
- Nead MA, Baglia LA, Antinore MJ, Ludlow JW, McCance DJ. Rb binds c-Jun and activates transcription. *EMBO J* 1998; **17**: 2342–2352.
- Decary S, Decesse JT, Ogryzko V, Reed JC, Naugibneva I, Harel-Bellan A et al. The retinoblastoma protein binds the promoter of the survival gene bcl-2 and regulates its transcription in epithelial cells through transcription factor AP-2. *Mol Cell Biol* 2002; **22**: 7877–7888.
- Decesse JT, Medjkane S, Datto MB, Cremisi CE. RB regulates transcription of the p21/WAF1/CIP1 gene. *Oncogene* 2001; **20**: 962–971.
- Nam EH, Lee Y, Park YK, Lee JW, Kim S. ZEB2 upregulates integrin alpha 5 expression through cooperation with Sp1 to induce invasion during epithelial-mesenchymal transition of human cancer cells. *Carcinogenesis* 2012; **33**: 563–571.
- Van Aken EH, Papeleu P, De Potter P, Bruyneel E, Philippe J, Seregard S et al. Structure and function of the N-cadherin/catenin complex in retinoblastoma. *Invest Ophthalmol Vis Sci* 2002; **43**: 595–602.
- Kashima T, Kawaguchi J, Takeshita S, Kuroda M, Takanashi M, Horiuchi H et al. Anomalous cadherin expression in osteosarcoma—possible relationships to metastasis and morphogenesis. *Am J Pathol* 1999; **155**: 1549–1555.
- Rodriguez-Salas N, Palacios J, de Castro J, Moreno G, Gonzalez-Baron M, Gamallo C. Beta-catenin expression pattern in small cell lung cancer: correlation with clinical and evolutive features. *Histol and Histopathol* 2001; **16**: 353–358.
- Sosa-Garcia B, Gunduz V, Vazquez-Rivera V, Cress WD, Wright G, Bian H et al. A role for the retinoblastoma protein as a regulator of mouse osteoblast cell adhesion: implications for osteogenesis and osteosarcoma formation. *PLoS One* 2010; **5**: 11.
- Guo WJ, Giancotti FG. Integrin signalling during tumour progression. *Nat Rev Mol Cell Biol* 2004; **5**: 816–826.
- Barczyk M, Carracedo S, Gullberg D. Integrins. *Cell Tissue Res* 2010; **339**: 269–280.
- Camper L, Hellman U, Lundgren-Akerlund E. Isolation, cloning, and sequence analysis of the integrin subunit alpha10, a beta1-associated collagen binding integrin expressed on chondrocytes. *J Biol Chem* 1998; **273**: 20383–20389.
- Camper L, Holmvalk K, Wangnerud C, Aszodi A, Lundgren-Akerlund E. Distribution of the collagen-binding integrin alpha10beta1 during mouse development. *Cell Tissue Res* 2001; **306**: 107–116.
- Varas L, Ohlsson LB, Honeth G, Olsson A, Bengtsson T, Wiberg C et al. Alpha10 integrin expression is up-regulated on fibroblast growth factor-2-treated mesenchymal stem cells with improved chondrogenic differentiation potential. *Stem Cells Dev* 2007; **16**: 965–978.
- Bengtsson T, Aszodi A, Nicolae C, Hunziker EB, Lundgren-Akerlund E, Fassler R. Loss of alpha10beta1 integrin expression leads to moderate dysfunction of growth plate chondrocytes. *J Cell Sci* 2005; **118**(Pt 5): 929–936.
- Croxton R, Ma Y, Cress WD. Differences in DNA binding properties between E2F1 and E2F4 specify repression of the Mcl-1 promoter. *Oncogene* 2002; **21**: 1563–1570.
- Stark C, Breitkreutz BJ, Chait-Aryamontri A, Boucher L, Oughtred R, Livstone MS et al. The BioGRID Interaction Database: 2011 update. *Nucleic Acids Res* 2011; **39**, Database issue D698–D704.
- Cartharius K, Frech K, Grote K, Klocke B, Haltmeier M, Klingenhoff A et al. MatInspector and beyond: promoter analysis based on transcription factor binding sites. *Bioinformatics* 2005; **21**: 2933–2942.
- Quandt K, Frech K, Karas H, Wingender E, Werner T. MatInd and MatInspector: new fast and versatile tools for detection of consensus matches in nucleotide sequence data. *Nucleic Acids Res* 1995; **23**: 4878–4884.
- Wan X, Kim SY, Guenther LM, Mendoza A, Briggs J, Yeung C et al. Beta4 integrin promotes osteosarcoma metastasis and interacts with ezrin. *Oncogene* 2009; **28**: 3401–3411.
- Richardson AL, Wang ZGC, De Nicolo A, Lu X, Brown M, Miron A et al. X chromosomal abnormalities in basal-like human breast cancer. *Cancer Cell* 2006; **9**: 121–132.

23. Haqq C, Nosrati M, Sudilovsky D, Crothers J, Khodabakhsh D, Pulliam BL *et al*. The gene expression signatures of melanoma progression. *Proc Natl Acad Sci U S A* 2005; **102**: 6092–6097.
24. Hou J, Aerts J, den Hamer B, van IJcken W, den Bakker M, Riegman P *et al*. Gene expression-based classification of non-small cell lung carcinomas and survival prediction. *PLoS One* 2010; **5**: 4.
25. Dyrskjot L, Kruhoffer M, Thykjaer T, Marcussen N, Jensen JL, Moller K *et al*. Gene expression in the urinary bladder: a common carcinoma *in situ* gene expression signature exists disregarding histopathological classification. *Cancer Res* 2004; **64**: 4040–4048.
26. Jones J, Otu H, Spentzos D, Kolia S, Inan M, Beecken WD *et al*. Gene signatures of progression and metastasis in renal cell cancer. *Clin Cancer Res* 2005; **11**: 5730–5739.
27. Landi MT, Dracheva T, Rotunno M, Figueroa JD, Liu H, Dasgupta A *et al*. Gene Expression Signature of Cigarette Smoking and Its Role in Lung Adenocarcinoma Development and Survival. *PLoS One* 2008; **3**: 2.
28. Kaiser S, Park YK, Franklin JL, Halberg RB, Yu M, Jessen WJ *et al*. Transcriptional recapitulation and subversion of embryonic colon development by mouse colon tumor models and human colon cancer. *Genome Biol* 2007; **8**: 7.
29. Sellers WR, Novitch BG, Miyake S, Heith A, Otterson GA, Kaye FJ *et al*. Stable binding to E2F is not required for the retinoblastoma protein to activate transcription, promote differentiation, and suppress tumor cell growth. *Genes Dev* 1998; **12**: 95–106.
30. Johnson JL, Pillai S, Pernazza D, Sebt SM, Lawrence NJ, Chellappan SP. Regulation of matrix metalloproteinase genes by E2F transcription factors: Rb–Raf-1 interaction as a novel target for metastatic disease. *Cancer Res* 2012; **72**: 516–526.
31. Wang CG, Hou XH, Mohapatra S, Ma YH, Cress WD, Pledger WJ *et al*. Activation of p27(Kip1) expression by E2F1—A negative feedback mechanism. *J Biol Chem* 2005; **280**: 12339–12343.
32. Knudsen ES, Wang JY. Dual mechanisms for the inhibition of E2F binding to RB by cyclin-dependent kinase-mediated RB phosphorylation. *Mol Cell Biol* 1997; **17**: 5771–5783.
33. He Y, Armanious MK, Thomas MJ, Cress WD. Identification of E2F-3B, an alternative form of E2F-3 lacking a conserved N-terminal region. *Oncogene* 2000; **19**: 3422–3433.
34. Ghosh N, Gyory I, Wright G, Wood J, Wright KL. Positive regulatory domain I binding factor 1 silences class II transactivator expression in multiple myeloma cells. *J Biol Chem* 2001; **276**: 15264–15268.
35. Flores AM, Kassatly RF, Cress WD. E2F-3 accumulation is regulated by polypeptide stability. *Oncogene* 1998; **16**: 1289–1298.
36. Chen L, Chen DT, Kurtyka C, Rawal B, Fulp WJ, Haura EB *et al*. Tripartite motif containing 28 (Trim28) can regulate cell proliferation by bridging HDAC1/E2F interactions. *J Biol Chem* 2012; **287**: 40106–40118.
37. Hazlehurst LA, Valkov N, Wisner L, Storey JA, Boulware D, Sullivan DM *et al*. Reduction in drug-induced DNA double-strand breaks associated with beta1 integrin-mediated adhesion correlates with drug resistance in U937 cells. *Blood* 2001; **98**: 1897–1903.
38. Eschrich SA, Hoerter AM. Libaffy: software for processing Affymetrix GeneChip data. *Bioinformatics* 2007; **23**: 1562–1564.



Cell Death and Disease is an open-access journal published by **Nature Publishing Group**. This work is licensed under a **Creative Commons Attribution-NonCommercial-ShareAlike 3.0 Unported License**. To view a copy of this license, visit <http://creativecommons.org/licenses/by-nc-sa/3.0/>